Prediction of Fetal Acidemia based on the Very Low Frequency Components of the Fetal Heart Rate and Fetal Pulse Oximetry recordings during Labor

G. Vasios, A. Prentza, E. Sifakis, P. Thomopoulos, E. Salamalekis and D. Koutsouris

Abstract—**The objective of the present study is the prediction of fetal acidemia based on the Very Low Frequency (VLF) components of the Fetal Heart Rate (FHR) and Fetal Pulse Oximetry ($FspO_2$) recordings during labor. In order to perform the spectral analysis, we applied the Continuous Wavelet Transform (CWT) and the adaptive approximation technique using the Matching Pursuit (MP) algorithm. The evaluation of $FspO_2$ was based on calculating the time duration in which the $FSpO_2$ was less than 30% ($T_{SpO2<30\%}$). We demonstrate that the oscillating activity of the FHR of about 0.01 Hz identified by the MP method and the $T_{SpO2<30\%}$ parameter, show an adequate sensitivity (90%) in predicting fetal acidemia, whereas the combination of these two variables shows a very good specificity (94%). The results of the analysis of our data demonstrate that the analysis of the fetal heart rate by the matching pursuit and the fetal pulse oximetry recordings may provide additional source of information about fetal status and to alert the clinician to decide under objective conditions when and how to perform the delivery**

I. Introduction

DURING the last decades, Fetal Heart Rate (FHR) monitoring has been widely used for intra- and antepartum monitoring and assessment of fetal well-being. It is commonly used as a screening modulus of the fetes to detect in advance possible fetal problems that could result in irreversible neurological damage or even fetal death during labor.

Although these methods have been proved to be a useful tool for the obstetricians, suspicious FHR patterns lack specificity and false positive FHR traces may result in unnecessary intervention increasing the caesarian section delivery rate. Moreover, there are cases in which the difference between inter and intra interpretations of the FHR patterns could be very large indicating the need of the development of methods that could provide more objective and quantitative analysis of the FHR traces and the application of non-invasive techniques such as the reflectance pulse oximetry as an additional source of information about fetal status, in order to prevent fetal hypoxia. Much research has gone into evaluating Fetal Pulse Oximetry ($FSpO_2$), its safety, accuracy and reliability in predicting neonatal outcome [1].

In recent years, several attempts have been made to automate the diagnosis of the fetal status. Computerized algorithms, artificial neural networks and hybrid architectures have been developed and validated in order to assess the fetal heart rate parameters (baseline of the fetal heart rate, accelerations and decelerations, etc.) and to predict fetal acidemia. Our method is based on the Very Low Frequency (VLF) oscillatory components of the FHR and the statistical analysis of the $FSpO_2$.

The motivation of using the VLF components of the FHR, (especially the long term slowly varying fluctuations in the frequency range between 0.008-0.015 Hz, VLF_I), as one of the predictive parameters of fetal acidemia, was based on our previous study [2]. According to this study, we demonstrated that when there was a reduction of umbilical artery pH and an increase in base deficit there was an increase of this kind of oscillations.

In order to evaluate this kind of activity, we applied the Wavelet Transform (WT) and the Matching Pursuit method (MP), since the fetal heart rate is a highly nonstationary signal and the traditional method of the Short-Time Fourier Transform (STFT) may eliminate the effects of nonstationarity, which occur at the expense of low frequency and time localization. Both WT and MP revealed the same results.

In general, the Wavelet Transform has proved to be one of the most successful techniques for the analysis of signals, even when nonstationarities are present, and it is able to localize the signal more accurately both in time and frequency domains. This method has rendered many successful applications in the area of biomedical signal processing [3] - [5] and has been used by Stefanovska et al. [6] and Lotrič et al. [7] in order to determine the spectral components of various biological signals.

The Matching Pursuit is an adaptive method which exhibits high time-frequency resolution, provides time-frequency representations of the signal's energy without cross-terms, has the ability to identify multiple periodicities in a highly nonstationary signal and has been widely used in order to extract time-frequency patterns of various biological signals [5], [8]-[12].

The objective of the present study is to estimate the prediction of fetal acidemia based on: 1) the oscillating activity of the FHR in the frequency range 0.008-0.015 Hz obtained by the WT and the MP and 2) on the same parameters in conjunction with the $FSpO_2$ (taken as a threshold value for $FSpO_2$ measurement the 30% level)

during the second stage of labor.

II. Methodology

A. Data Collection

The investigation was performed on seventy-three (73) fetuses of more than thirty-seven (37) weeks gestation, which were monitored throughout labor in the Labor Ward of the 3rd University Clinic of Obstetrics and Gynecology at Attikon Hospital of Athens. All women gave informed consent to this study, which was also approved by the Ethics Committee of the Attikon Hospital. Women with antepartum metabolic or endocrine disorders were not included in the study. Ten (10) cases, in which umbilical artery pH was lower than 7.15 ($7.00 \le$ pHumb.art < 7.15, highly increased concentration of hydrogen ions in blood) and base deficit was lower than –8 mM/l formed the acidemic group according to Strachan et al. [13]. The rest of the fetuses formed the normal group.

The Cardiotocogram (CTG) was recorded during labor using the Corometrics Series 120 Cardiotocograph. FHR was measured externally. A transducer placed on the mother's abdomen was used to direct an ultrasonic beam toward the fetal heart and to sense Doppler shifted echoes created by moving cardiac structures. FHR recordings were fed into a personal computer with a sampling frequency of 1Hz. The last thirty (30) minutes segments before delivery were analyzed and artifacts and abrupt changes were removed manually.

The percentage of the functional oxygen saturation of fetal arterial blood ($FSpO_2$) was measured non-invasively by applying the Nellcor Puritan Benett fetal oxygen sensor to the cheek/temple area of the fetal head. Abrupt changes of $FSpO_2$ were removed and linear interpolation was employed, when the duration of the artifact was below a certain value.

B. Continuous Wavelet Transform

Wavelet analysis is a scale-independent method. It involves the representation of a time function in terms of simple fixed building blocks termed wavelets. These building blocks are actually a family of functions, which are derived from a single generating function called the mother wavelet $\psi(t)$ by translation and dilation operations creating a family of functions:

$$\psi_{s,u}(t) = \frac{1}{\sqrt{s}}\psi\left(\frac{t-u}{s}\right) \tag{1}$$

The parameter s is a scaling factor and stretches or compresses the mother wavelet. The parameter u is a translation along the time axis and simply shifts a wavelet and so delays or advances the time at which it is activated. The factor $1\sqrt{s}$ is used to ensure that the wavelets at every scale all have the same energy. The stretched and compressed wavelets through scaling operation are used to capture the different frequency components of the function being analyzed. The translation operation, on the other hand, involves shifting of the mother wavelet along the time axis to capture the time information of the function to be analyzed at a different position. In this way, a family of scaled and translated wavelets can be created using scaling and translation parameters s and u.

The Continuous Wavelet Transform (*CWT*) of a signal $x(t)$ is defined as:

$$CWT(s,u) = \frac{1}{\sqrt{s}}\int_{-\infty}^{\infty} x(t)\psi^*\left(\frac{t-u}{s}\right)dt \tag{2}$$

where * is the complex conjugation. The wavelet transform $CWT(s,u)$ is a mapping of the function $\psi(t)$ onto the time-scale plane. The function can be recovered from $CWT(s,u)$ by:

$$x(t) = C^{-1}\int_0^{\infty}\int_{-\infty}^{\infty}|s|^{2p-3}\,CWT(s,u)\psi_{s,u}(t)\,ds\,du \tag{3}$$

where the constant C is determined by the shape of the mother wavelet. The reconstruction is possible only if $0 < C < \infty$ and in this case the mother wavelet is admissible. Using the reconstruction formula and the wavelet properties, the following expression for the total energy of the signal $x(t)$ is obtained:

$$\|x(t)\|^2 = C^{-1}\int_0^{\infty}\int_{-\infty}^{\infty}|s|^{2p-3}\,|CWT(s,u)|^2\,ds\,du \tag{4}$$

The function:

$$\varepsilon_W(s,u) = C^{-1}|s|^{2p-3}\,|CWT(s,u)|^2 \tag{5}$$

can therefore be interpreted as the two-dimensional wavelet energy density function of the signal in the time-scale plane. It is often called scalogram. The interpretation of $\varepsilon_W(s,u)$ depends on the mother wavelet being used. To detect the frequency content in a given time interval, a mother wavelet that is well concentrated in both time and frequency must be used. All functions obey the uncertainty principle which states that sharp localization in time and frequency are mutually exclusive. The time (Δt) and frequency ($\Delta\omega$) resolutions are connected by $\Delta t\Delta\omega \ge c$, where c is a constant. The equality is attained only for a Gaussian function [14].

The Morlet wavelet is the most commonly used complex wavelet. It is a Gaussian function modulated with a sine wave with basic frequency $\omega_0=2\pi f_0$. In the time domain, it is written as:

$$\psi(t) = \frac{1}{\sqrt[4]{\pi}}\left(e^{-i\omega_0 t} - e^{-\omega_0^2/2}\right)e^{-t^2/2} \tag{6}$$

The choice of ω_0 is a compromise between localizations in time and in frequency. The function given by equation (6) is not really a wavelet as it has a non-zero mean, i.e. the zero frequency term of its corresponding energy spectrum is non-zero and hence it is inadmissible. However, for $\omega_0 > 5$, the value of the second term in (6) is so small that it can be ignored in practice with minimal error and a simplified expression for the Morlet wavelet in the time domain is:

$$\psi(t) = \frac{1}{\sqrt[4]{\pi}} e^{-i\omega_0 t} e^{-t^2/2} \tag{7}$$

C. Matching Pursuit Method

A nonstationary signal can be expanded into waveforms (called atoms) whose time-frequency properties can be adapted to its local structures. These waveforms are contained into a complete redundant dictionary. A general family of time-frequency atoms can be generated by scaling, translating and modulating a single window function $g(t)$ [15],[16]. For any scale $s > 0$, frequency modulation ω and translation u, we denote $\gamma = (s, u, \omega)$ and define the atom as:

$$g_\gamma(t) = \frac{1}{\sqrt{s}} g\left(\frac{t-u}{s}\right) e^{i\omega t} \tag{8}$$

The factor $1/\sqrt{s}$ normalizes to 1 the norm of $g_\gamma(t)$. The window function $g(t)$ is usually even and its energy is mostly concentrated in a neighborhood of u, whose size is proportional to s. In frequency domain, the energy is mostly concentrated around ω with a spread proportional to $1/s$. The minimum of the time-frequency variance is obtained when $g(t)$ is Gaussian (Gabor atom). The dictionaries of windowed Fourier transform and wavelet transform can be derived as subsets of this dictionary, defined by certain restrictions on the choice of parameters. In the case of the windowed Fourier transform, the scale s is constant – equal to the window length – and the parameters ω and u are uniformly sampled. In the case of the wavelet transform, the frequency modulation is limited by the restriction on the frequency parameter $\omega = \omega_0/s$, ω_0 = constant. Thus, the Gabor atom used in the matching pursuit method is more flexible in that its scale, location and internal frequency may all be varied independently.

In order to decompose a signal $x(t)$ into a set of atoms which can best describe the time-frequency structure of the signal, an iterative orthogonal projection of $x(t)$ onto the dictionary is necessary. In the first step of the iterative procedure we choose the vector $g_{\gamma 0}(t)$ which gives the largest product with the signal $x(t)$:

$$x(t) = \langle x(t), g_{\gamma 0}(t) \rangle g_{\gamma 0}(t) + R^1 x(t) \tag{9}$$

where the first term in the right-hand side of the above equation is the projection of $x(t)$ onto the atom $g_{\gamma 0}(t)$ and the second term $R^1 x(t)$ is the residual vector after approximating $x(t)$ in the direction of $g_{\gamma 0}(t)$. After this first step, the iterative procedure is repeated on the following obtained residues:

$$R^i x(t) = \langle R^i x(t), g_{\gamma i}(t) \rangle g_{\gamma i}(t) + R^{i+1} x(t) \tag{10}$$

In this way the signal $x(t)$ is decomposed into a sum of time-frequency atoms chosen to match optimally the signal's residues, and if this procedure is repeated until the signal is decomposed into m components, $x(t)$ is represented as:

$$x(t) = \sum_{i=0}^{m-1} \left\langle R^i x(t), g_{\gamma i}(t) \right\rangle g_{\gamma i}(t) + R^m x(t) \tag{11}$$

and its energy is given by:

$$\|x(t)\|^2 = \sum_{i=0}^{m-1} \left| \left\langle R^i x(t), g_{\gamma i}(t) \right\rangle \right|^2 + \left\| R^m x(t) \right\|^2 \tag{12}$$

where $R^i x(t)$ is the signal residue for the ith iteration and $R^0 x(t) = x(t)$.

It can be shown [15] that as m $\to \infty$, the signal can be represented as an infinite series of time-frequency atoms from the dictionary without any distortion:

$$x(t) = \sum_{i=0}^{\infty} \left\langle R^i x(t), g_{\gamma i}(t) \right\rangle g_{\gamma i}(t)$$
$$\lim_{m \to \infty} R^m x(t) = 0 \tag{13}$$

and the energy of the signal is:

$$\|x(t)\|^2 = \sum_{i=0}^{\infty} \left| \left\langle R^i x(t), g_{\gamma i}(t) \right\rangle \right|^2 \tag{14}$$

Although this decomposition is nonlinear, we have energy conservation as if it was a linear orthogonal decomposition. The matching pursuit method finds the time-frequency atoms in a decreasing energy order and the higher energy components of the signal are always extracted first. These higher energy components are regarded as the coherent part of the signal due to the similarity between their waveforms and the signal.

To illustrate decomposition into time-frequency atoms, we compute its energy density defined by:

$$\varepsilon_{MP}(t, \omega) = \sum_{i=0}^{m-1} \left| \left\langle R^i x(t), g_{\gamma i}(t) \right\rangle \right|^2 W g_{\gamma i}(t, \omega) \tag{15}$$

where $Wg_{\gamma i}$ is the Wigner distribution of atom $g_{\gamma i}(t,\omega)$.

Unlike the Wigner and the Cohen class distributions, the time-frequency energy distribution revealed by MP does not include cross terms.

III. Data Processing

A. Wavelet Transform Analysis of the Fetal Heart Rate Signals

In order to apply the CWT, we used software written in Matlab (The MathWorks Inc.) and provided by [17]. An approximation of the continuous wavelet transform was calculated for the last 30 min of the normalized FHR signal during labor (each FHR signal was normalized by its standard deviation). In our implementation, the Morlet mother wavelet was chosen with $\omega_0 = 6$ to perform the transform, while the scales s were chosen arbitrarily to be fractional powers of two:

$$s_j = s_0 2^{j\delta j}, \; j = 0,1,\ldots,J$$
$$J = \delta j^{-1} \log_2 (N\delta t / s_0) \quad (16)$$

where s_0 is the smallest resolvable scale, J determines the largest scale, δj is the spacing between the discrete scales, δt the time spacing (inverse of sampling frequency) and N the number of samples. s_0 was chosen so that the equivalent Fourier period is approximately $2\delta t$, since the smallest scale that can be resolved is approximately equal to the Nyquist frequency. Since smaller values of δj give a finer resolution, the value of 0.1 was used for δj in this study. By choosing $\omega_0 = 6$, the relationship between scale and frequency is simple and can be obtained by the equality $\lambda = 1.03s$, where λ is the equivalent Fourier period, indicating that for the Morlet wavelet the wavelet scale is almost equal to the Fourier period [17]. This is a reasonable choice for ω_0, since we prefer to detect the frequency content of the FHR. The frequency resolution changes with frequency: at low frequencies (large scales) the resolution is better than at high frequencies (small scales). Accordingly, the time resolution is better for high than it is for low frequency components.

Based on the local minima of the time averaged wavelet transform two frequency intervals were determined, interval I (0.008-0.015 Hz) and interval II (0.015-0.04 Hz) and the contribution of each peak or each spectral component can be characterized by the time average energy density, P_{Wi}, of the corresponding interval i:

$$P_{Wi}(f_{i1}, f_{i2}) = \frac{1}{T}\int_0^T \int_{1/f_{i1}}^{1/f_{i2}} \frac{1}{s^2} |CWT(s,u)|^2 \, dsdu \quad (17)$$

where T is the time duration of the FHR signal and $p = 1/2$ was chosen in equation (3).

B. Adaptive Approximation Analysis of the Fetal Heart Rate Signals

In order to get a decomposition of the normalized FHR signals with real expansion coefficients and real residuals, real-only atoms are used of the form:

$$g_{\gamma i}(t) = K_i \frac{2^{1/4}}{\sqrt{s_i}} e^{-\pi[(t-u_i)/s_i]^2} \cos(\omega_i t + \phi_i) \quad (18)$$

where s_i and u_i are the scale and location factors for the Gaussian envelope, ω_i and φ_i are respectively the frequency and phase of the real sinusoid within the Gaussian envelope and K_i is a normalization factor used to maintain unit energy for $g_{\gamma i}(t)$. We used a dictionary composed of discrete Gabor functions supplemented with canonical basis of discrete Dirac functions and discrete Fourier basis. In this case we denote $\gamma=(s,u,2\pi k/N)$, where N is the number of the samples of the signal, u and k are integers between 0 and N and $\varphi \in [0,2\pi]$. In order to reduce the computation, the scale s is also limited to an exponential relation $s = 2^j$ where j is the octave of the scale s which varies between zero and $\log_2 N$. Therefore, the signal duration was always zero-padded to a power of two in our case, resulting to 2048 signal points.

Since the decomposition itself does not set the number of iterations to perform, but sort atoms by largest inner product with residual, in our implementation in order to get the best way to decompose the signal, we studied the residual log-energy ($\log_{10}||R^i x||/||x||$) as a function of the number of time-frequency atoms (i.e., the algorithm's iterations). This magnitude provides some help in order to get the best way to decompose the signal. When it has a relative fast decay for a number of iterations, these iterations, i.e. atoms, correspond to the coherent signal structures. On the other hand, when its decay reaches a linear behavior, which means that the decay of $||R^i x||$ is almost constant, then there are no more structures in the residuum coherent with the chosen directory and the time-frequency energy distribution map becomes very noisy and complicated with confusing structures, without providing information about the most energetic components of the decomposed signal. For each FHR segment we studied the decay rate of the residual log-energy for a predefined number (M=500) of algorithm's iterations. For all the cases we noticed that by selecting the energy of the residue to be equal to the 5% of the total energy of the original FHR signal the residual log-energy function does not reaches its linear behavior. Thus, the number of the atoms that has been taken into account in order to decompose each FHR segment was $m_{0.95}$:

$$0.95 \le \sum_{i=0}^{m_{0.95}-1} \frac{\|c_i\|^2}{\|x\|^2} \quad \text{and} \quad 0.95 > \sum_{i=0}^{m_{0.95}-2} \frac{\|c_i\|^2}{\|x\|^2} \quad (19)$$

where $c_i = \langle R^i x, g_{\gamma i} \rangle$ and the square of c_i represents the part of the signal energy associated with atom $g_{\gamma i}$. Each fetal heart rate segment is decomposed by $m_{0.95}$ atoms. This number is

not necessarily the same for the FHR segments, since it depends on the amount of information contained in the signal and the coherence with the chosen dictionary.

The Last Wave software package [18] was used for applying the MP algorithm.

Since the aim of the present study is to estimate the prediction of fetal acidemia based on the oscillating dynamics of fetal heart rate variability in the very low frequency range we confined our study to the rhythmic and sinusoidal waveforms bellow 0.04 Hz. In order to quantify the VLF oscillating components, we estimated the total energy of all the atoms representing the corresponding activity between 0.008 and 0.04 Hz (TE_{MP_VLF}) and between the two sub-intervals 0.008-0.015 Hz (TE_{MP_I}) and 0.015-0.04 Hz (TE_{MP_II}) for each case.

C. Analysis of the $FSpO_2$

For each 30-minute segment, we calculated the total time in which the $FSpO_2$ was less than 30% ($T_{SpO2<30\%}$) [19].

IV. Results

The significance of the difference between the acidemic and the normal group was evaluated using the Student's t-test. As a criterion of significance, the 95% confidence level ($p < 0.05$) was chosen.

In order to assess the usefulness of the quantities P_{W_I}, TE_{MP_I} (since in our previous study [2] we demonstrated that these parameters were significantly increased in the acidemic group) and $T_{SpO2<30\%}$, as predictors of acidemia, we calculated the sensitivity, specificity, positive predictive value, negative predictive value, likelihood ratio and the area under the receiver operating characteristic curve.

Moreover, in order to categorize our data based on the conjunction of two different parameters (P_{W_I} with $T_{SpO2<30\%}$, and TE_{MP_I} with $T_{SpO2<30\%}$), we used the K-means clustering algorithm.

TABLE I
PREDICTIVE VALUE OF THE PARAMETRES P_{W_I}, TE_{MP_I} AND $T_{SpO2<30\%}$

	P_{W_I}	TE_{MP_I}	$T_{SpO2<30\%}$
Sensitivity (%)	80	90	90
Specificity (%)	61	87	81
PPV (%)	25	53	43
NPV (%)	95	98	98
Likelihood ratio	2.0	7.1	4.7
AUC ± S.E	0.72±0.09	0.93±0.06	0.88±0.07

PPV: Positive Predictive Value, NPV: Negative Predictive Value, AUC: Area under receiver operating characteristic Curve, S.E.: Standard Error

TABLE II
PREDICTIVE VALUE OF THE PARAMETRES P_{W_I} WITH $T_{SpO2<30\%}$ AND TE_{MP_I} WITH $T_{SpO2<30\%}$

	P_{W_I} with $T_{SpO2<30\%}$	TE_{MP_I} with $T_{SpO2<30\%}$
Sensitivity (%)	60	80
Specificity (%)	89	94
PPV (%)	46	67
NPV (%)	93	97
Likelihood ratio	5.4	12.5

PPV: Positive Predictive Value, NPV: Negative Predictive Value

A. Results of each individual parameter as a predictor of acidemia

Table I shows the predictive value of each parameter. Both TE_{MP_I} and $T_{SpO2<30\%}$ showed an adequate ability to predict acidemia, with a higher value being associated with acidemia. The mean value and standard error of TE_{MP_I} and $T_{SpO2<30\%}$ were 220.4 ± 38.9 and 7.2 ± 1.6 min respectively for the acidemic group, and for the normal group 65.0 ± 9.9 and 1.2 ± 0.4 min respectively. The corresponding p-values were lower than 0.0001. The sensitivity and negative predictive value were high for these parameters, however the sensitivity of P_{W_I} was lower, although there was a significant difference between the two groups (p-value 0.002). About the specificity, TE_{MP_I} gives the better result (87%).

B. Results for each pair of parameters as a predictor of acidemia

Table II shows the predictive value of each pair of parameters. Figures 1 and 2 illustrate the corresponding scatter plots. Best results are obtained by the conjunction of TE_{MP_I} and $T_{SpO2<30\%}$. Although the sensitivity is decreased, the specificity is remarkably increased in relation to the corresponding values of TE_{MP_I} and $T_{SpO2<30\%}$.

V. Discussion

Fetal HRV is often used as an index of fetal health. We calculated the spectral estimations of the VLF oscillatory components of the complicated fetal heart rate by the continuous wavelet transform that provides variable time and scale resolution and the matching pursuit method which provides variable time, scale and frequency resolution. Both of these techniques indicate that the heart rate oscillations in the frequency range between 0.008-0.015 Hz are increased when the concentration of hydrogen ions in fetal blood is increased. However, as we have noticed, the MP method showed an adequate ability to predict acidemia due to the fact that it is superior to the WT in identifying rhythmical and sinusoidal oscillations of about 0.01 Hz of the highly nonstationary FHR, which are mainly associated with hormonal changes [6]. The corresponding oscillations reflect in the fetal heart rate the extent and the duration of some of the adaptive responses and oxygen transport

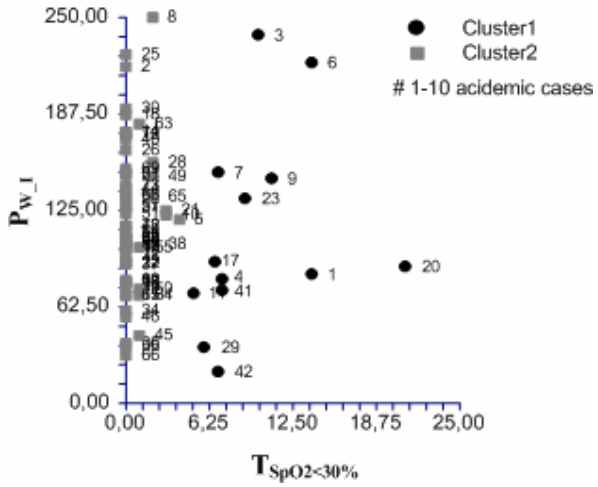

Fig. 1. Scatter plot of the variables P_{W_I} and $T_{SpO2<30\%}$. Numbers 1-10 correspond to acidemic cases. Cluster 1 contains 6 out of 10 acidemic cases and 7 out of 63 normal ones.

mechanisms of the fetus when it becomes acidemic.

Fetal pulse oximetry seems to be an important additional source of information. Taken as a threshold value for $FSpO_2$ measurement the 30% level and calculating the time duration in which the $FSpO_2$ was less than 30%, we obtained that the parameter $T_{SpO2<30\%}$ showed a high sensitivity and negative predictive value.

However, taking into account that one of the main problems of the obstetricians is that the suspicious FHR patterns lack specificity and the increased false positive rate may result in unnecessary interventions increasing the caesarian section delivery rate, it appears that the combination of $FSpO_2$ and the MP analysis of the FHR may help to overcome this problem, since it shows a very good specificity (94%).

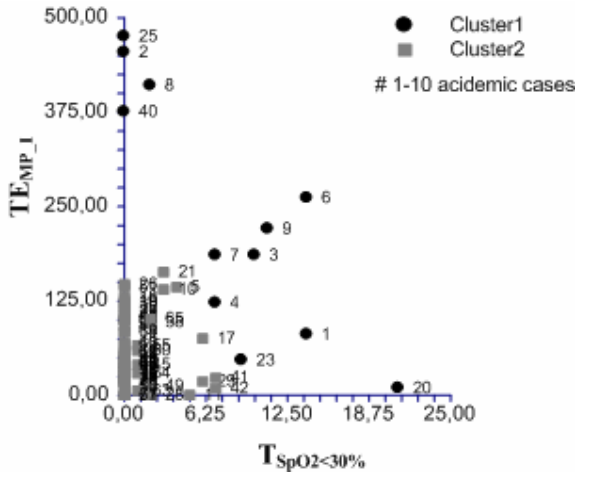

Fig. 2. Scatter plot of the variables TE_{MP_I} and $TSpO2_{<30\%}$. Numbers 1-10 correspond to acidemic cases. Cluster 1 contains 8 out of 10 acidemic cases and 4 out of 63 normal ones.

VI. Conclusion

The results of the analysis of our data demonstrate that the analysis of the fetal heart rate by the matching pursuit and the fetal pulse oximetry recordings may provide additional source of information about fetal status and to alert the clinician to decide under objective conditions when and how to perform the delivery. However, further evaluation is mandatory to evaluate its efficacy and reliability in order to be part of a system that could recognize early the fetal acidemia.

References

[1] J. Yam, S. Chua and S. Arulkumaran, "Intrapartum Fetal Pulse Oximetry. Part 2: Clinical Application," *CME Review Article, Obstet and Gynecol Survey*, vol. 55(3), pp. 173-183, 2000.

[2] G. Vasios, A. Prentza, E. Sifakis and D. Koutsouris, "Spectral estimation of the very low frequency components of the fetal heart rate during labor determined by continuous wavelet transform and matching pursuit," in *Proc. 2nd Int Conf. Comput. Intel. Medicine and Healthcare*, Lisbon, 2005, pp. 217-223.

[3] A. Aldroubi and M. Unser, *Wavelets in Medicine and Biology*, CRC Press, Boca Raton FL, 1996.

[4] M. Unser and A. Aldroubi, "A review of wavelets in biomedical applications," *Proc. IEEE*, vol. 84(4), pp. 626-638, 1996.

[5] M. Akay, *Time-Frequency and Wavelets in Biomedical Signal Processing*. NJ: IEEE Press, Piscataway, 1998.

[6] A. Stefanovska, M. Bračič and H.D. Kvernmo, "Wavelet Analysis of Oscillations Measured by Laser Doppler Technique," *IEEE Trans. Biomed. Eng*., vol. 46, pp. 1230-1239, 1999.

[7] M.B. Lotrič, A. Stefanovska, D. Štajer and V. Urbančič-Rova, "Spectral components of heart rate variability determined by wavelet analysis," *Physiol. Meas*., vol. 21, pp. 441-457, 2000.

[8] P.J. Durka, "From wavelets to adaptive approximations: time-frequency parametrization of EEG," *BioMed. Eng. Online*, vol. 2, pp. 1-30, 2003.

[9] M. Akay and J.A. Daubenspeck, "Investigating the Contamination of Electroencephalograms by Facial Muscle Electromyographic Activity Using Matching Pursuit," *Brain Lang*., vol. 66, pp. 184-200, 1999.

[10] X. Zhang, L-G. Durand, L. Senhadji, H.C. Lee and J-L. Coatrieux, "Time-Frequency Scaling Transformation of the Phonocardiogram Based of the Matching Pursuit Method, " *IEEE Trans. Biomed. Eng*, vol. 45, pp. 972-979, 1998.

[11] M. Akay and H.H. Szeto, "Analysis of Fetal Breathing Using Matching Pursuits," *IEEE EMB Magazine*, pp. 195-198, 1995.

[12] M. Akay and E. Mulder, "Examining Fetal Heart-Rate Variability Using Matching Pursuits," *IEEE EMB Magazine*, pp. 64-67, 1996.

[13] B. Strachan, D. Sahota, W.J. Wijngaarden, D.K. James and A.Z.M. Chang, "The fetal electrocardiogram: relationship with acidemia at delivery, " *Am J Obstet Gynecol*, vol. 182, pp. 603-606, 2000.

[14] G. Kaiser, *A Friendly Guide to Wavelets*. Boston, MA: Birkhäuser, 1994.

[15] S. Mallat and Z. Zhang, "Matching pursuits with time-frequency dictionaries," *IEEE Trans. Signal Processing*, vol. 41, pp. 3397-3415, 1993.

[16] S. Qian and D. Chen, "Signal representation using adaptive normalized Gaussian functions," *Signal Processing*, vol. 36, pp. 1-11, 1994.

[17] C. Torrence and G. Compo, "A practical guide to wavelet analysis," *Bul. Am. Met. Soc*., vol. 79, pp. 61-78, 1998. Wavelet software available at: http://paos.colorado.edu/research/wavelets.

[18] Last Wave software package 2.0. Available at: http://www.cmap.polytechnique.fr/~bacry/LastWave.

[19] Bloom S, Swindle R, Mcintire D, Leveno K. "Fetal pulse oximetry: duration and desaturation and intrapartum outcome," *Obstet Gynecol*, vol. 93, pp. 1036-1040, 1999.